

Design and implementation of a leader-follower cooperative control system for unmanned helicopters

Ben YUN¹, Ben M. CHEN¹, Kai Yew LUM², Tong H. LEE¹

(1. Department of Electrical & Computer Engineering, National University of Singapore, Singapore 117576;

2. Temasek Laboratories, National University of Singapore, Singapore 117508)

Abstract: In this paper, we present a full scheme for the cooperative control of multiple unmanned aerial vehicle (UAV) helicopters. We adopt the leader-follower pattern to maintain a fixed geometrical formation while navigating the UAVs following certain trajectories. More specifically, the leader is commanded to fly on some predefined trajectories, and each follower is controlled to maintain its position in formation using the measurement of its inertial position and the information of the leader position and velocity, obtained through a wireless modem. More specifications are made for multiple UAV formation flight. In order to avoid possible collisions of UAV helicopters in the actual formation flight test, a collision avoidance scheme based on some predefined alert zones and protected zones is employed. Simulations and experimental results are presented to verify our design.

Keywords: Unmanned aerial vehicles; Cooperative control; Flight formation; Collision avoidance

1 Introduction

Unmanned aerial vehicles, or commonly known as UAVs, are autonomous flying vehicles equipped with sensing devices and possibly weapons. They can be used to carry out tasks in dangerous situations, for example, reconnaissance over hostile territories or tracking battle damage of enemy targets (see, e.g., [1]). UAVs have many potential military and civil applications and are also of great scientific significance in academic research. However, the current UAVs tend to be complex, expensive, and often bulky. This has motivated the development of the coordinating control of low-cost UAVs in formation flight, in which a group of UAVs fly in a desired graphic formation. The advantages of formation flight have long been known. It is believed that the formation-flying cooperative behavior of birds can increase the efficiency of group performance. Military aircraft, ground units, and naval forces use this strategy to benefit from mutual protection, concentration of offensive power, and simplification of control (see, e.g., [2~6]).

The UAV research group at the National University of Singapore has successfully constructed a series of UAV helicopters, integrated from some hobby radio-controlled helicopters such as Raptor 90, and implemented fully autonomous flight tests that include hovering, waypoint trajectory tracking navigation, automatic take-off and landing (see [7~9]). It is natural for us to expand our research domain to the flight formation of multiple UAVs.

In this paper, we present a full scheme for the cooperative control of multiple UAV helicopters, including control system design and collision avoidance scheme. In our proposed formation flight strategy, we adopt the leader-follower pat-

tern to maintain a fixed geometrical formation while navigating the UAVs following certain trajectories. More specifically, the leader UAV is commanded to fly along some predefined trajectories, and each follower is controlled to maintain its position in formation using the measurement of its inertial position and the information of the leader position and velocity, obtained through a wireless modem. In order to avoid possible collisions of UAV helicopters in the actual formation flight test, a collision avoidance scheme based on some predefined alert zones and protected zones is employed. Other specifications for multiple UAV formation are also investigated. Simulations and experimental results are presented to verify our design.

2 Dynamic model of single UAV platform

We review in this section some results for modeling and control of small-scale helicopters. A linear model has been obtained using frequency-domain system identification methods. This model is valid for hovering and low-velocity maneuvers (see, e.g., Kim et al. [10]). A controller is used for waypoint navigation of a single UAV. This controller is used as the inner loop controller in the design of a formation flight controller. It is used to guarantee the asymptotic stability of the relative motion between the UAV and the surrounding air.

The dynamic transient response of the relative motion between the UAV and the surrounding air can be assumed to be much faster than that of the flight trajectories in conventional maneuvering (see Larson [11]). Based on this assumption a frequency domain identification technique is used to fit the model parameters. We have completed the

modeling and control of an UAV helicopter Raptor 90 as shown in Fig. 1.



Fig. 1 HeLion: a UAV helicopter with Raptor 90.

The model of the UAV is given by

$$\dot{x} = Ax + B\bar{u}, \quad (1)$$

where

$$x = (u \ v \ p \ q \ \phi \ \theta \ a_s \ b_s \ w \ r \ r_{fb})^T, \quad (2)$$

$$\bar{u} = (\delta_{lat} \ \delta_{lon} \ \delta_{col} \ \delta_{ped})^T, \quad (3)$$

$$A = \begin{bmatrix} X_u & 0 & 0 & 0 & 0 & -g & X_{a_s} & 0 & 0 & 0 & 0 \\ 0 & Y_v & 0 & 0 & 0 & g & 0 & Y_{b_s} & 0 & 0 & 0 \\ L_u & L_v & 0 & 0 & 0 & 0 & L_{a_s} & L_{b_s} & 0 & 0 & 0 \\ M_u & M_v & 0 & 0 & 0 & 0 & M_{a_s} & M_{b_s} & 0 & 0 & 0 \\ 0 & 0 & 1 & 0 & 0 & 0 & 0 & 0 & 0 & 0 & 0 \\ 0 & 0 & 0 & 1 & 0 & 0 & 0 & 0 & 0 & 0 & 0 \\ 0 & 0 & 0 & -1 & 0 & 0 & \frac{-1}{\tau_f} & A_{b_s} & 0 & 0 & 0 \\ 0 & 0 & -1 & 0 & 0 & 0 & B_{a_s} & \frac{-1}{\tau_f} & 0 & 0 & 0 \\ 0 & 0 & 0 & 0 & 0 & 0 & Z_{a_s} & Z_{b_s} & Z_w & Z_r & 0 \\ 0 & 0 & N_p & 0 & 0 & 0 & 0 & 0 & N_w & N_r & N_{r_{fb}} \\ 0 & 0 & 0 & 0 & 0 & 0 & 0 & 0 & 0 & K_r & K_{r_{fb}} \end{bmatrix}, \quad (4)$$

$$B = \begin{bmatrix} \mathbf{0}_{6 \times 4} \\ A_{u_{a_s}} & A_{u_{b_s}} & 0 & 0 \\ B_{u_{a_s}} & B_{u_{b_s}} & 0 & 0 \\ 0 & 0 & Z_u & 0 \\ 0 & 0 & N_u & N_u \\ 0 & 0 & 0 & 0 \end{bmatrix}, \quad (5)$$

and where u , v , and w are the longitudinal, lateral, and vertical speeds (in m/s) in the helicopter coordinate frame; p , q , and r are the roll, pitch, and yaw rates (in rad/s) in the helicopter frame; ϕ and θ are the roll and pitch of the helicopter (in rad); a_s and b_s are the longitudinal and lateral rotor flapping angles; r_{fb} is a yaw rate feedback term in the dynamics; δ_{lat} and δ_{lon} correspond to the cyclic lateral and longitudinal control inputs; and δ_{col} and δ_{ped} are the collective and directional inputs, respectively. Interested readers are referred to [8] for more detailed information on matrices A and B . A flight control law designed using the so-called composite nonlinear feedback control technique has also been reported in [8]. The control system has been experimentally tested and proved to be very successful.

3 Modeling and control of flight formation

In this work, we focus primarily on a leader-follower formation flight pattern, in which one of the UAVs serves as the leader and the rest as the followers. In what follows, we present the dynamic model of such a formation scheme and its control law design.

3.1 Model of leader-follower formation flight

The position and altitude of the wind frame for both leader and follower UAVs need to be related to an inertial reference frame, denoted with the subscript as depicted in Fig. 2. To simplify the analysis, all the vectors \vec{R}_L , \vec{R}_W and \vec{R}_{LW} and the follower UAV's velocity are resolved in or transferred to leader UAV's wind frame (see [12]).

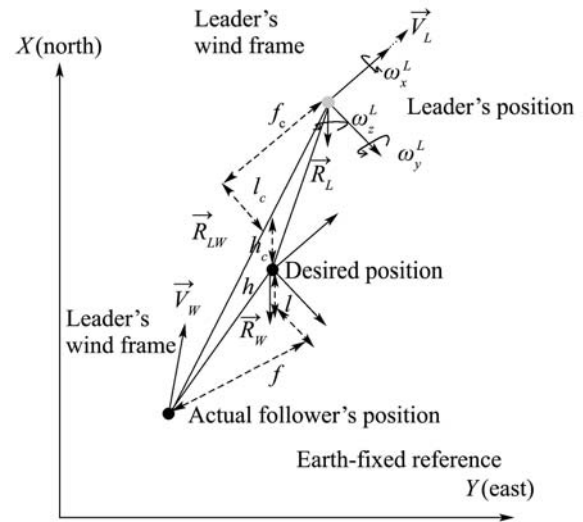


Fig. 2 Leader-follower UAV formation geometry.

The separation distance is also defined along the leader UAV's wind frame. Define f as positive when the follower is in the front of the desired position along the leader's velocity, which is the same as the definition of the x axis of the leader's wind frame; define l as positive when the follower is on the left side of the desired position, which is the same as the definition of the y axis of the leader's wind frame; define h as positive when the follower is under the desired position, which is the same as the definition of the z axis of the leader's wind frame. Then through the coordinate transformation to the leader UAV's wind frame, we have a direct geometric relation of the separation between the leader and the wing as follows:

$$\vec{R}_W = \vec{R}_{LW} - \vec{R}_L = \begin{pmatrix} f \\ l \\ h \end{pmatrix}, \quad (6)$$

where

$$\vec{R}_L = \begin{pmatrix} f_c \\ l_c \\ h_c \end{pmatrix}, \quad \vec{R}_{LW} = C_B \begin{pmatrix} x_L - x_w \\ y_L - y_w \\ z_L - z_w \end{pmatrix}, \quad (7)$$

and where matrix C_B is the transformation matrix from the NED frame to the leader's wind frame.

The leader UAV is flying at a velocity of V_L which rotates with an angular rate of ω_L , which drives the leader UAV's wind frame also rotating compared with the inertial frame.

The wind frame's rotating angular velocity, $\vec{\omega}_L$, is defined as

$$\vec{\omega}_L = \begin{pmatrix} \omega_x^L \\ \omega_y^L \\ \omega_z^L \end{pmatrix}. \quad (8)$$

From GPS signals, we can also calculate the transformation matrix from the NED frame to the leader UAV's wind frame [12], i.e.,

$$\cos \phi = \frac{V_x}{\sqrt{V_x^2 + V_y^2 + V_z^2}}, \quad (9)$$

$$\cos \theta = \frac{V_y}{\sqrt{V_x^2 + V_y^2 + V_z^2}}, \quad (10)$$

$$\cos \psi = \frac{V_z}{\sqrt{V_x^2 + V_y^2 + V_z^2}}, \quad (11)$$

where θ, ϕ, ψ are Euler angles between the NED frame and the leader UAV's wind frame. The transformation matrix from the NED frame to the leader UAV's wind frame is given by

$$B_{WL} = \begin{bmatrix} c\theta c\psi & c\theta s\psi & -s\theta \\ -c\phi s\psi + s\phi s\theta c\psi & c\phi c\psi + s\phi s\theta s\psi & s\phi c\theta \\ s\phi s\psi + c\phi s\theta c\psi & -s\phi c\psi + c\phi s\theta s\psi & c\phi c\theta \end{bmatrix},$$

where c and s denote \cos and \sin , respectively.

Noting that

$$\begin{aligned} \vec{R}_{W} &= \begin{pmatrix} f \\ l \\ h \end{pmatrix} \\ &= \vec{R}_{LW} - \vec{R}_L \\ &= B_{WL} \begin{pmatrix} x_L - x_w \\ y_L - y_w \\ z_L - z_w \end{pmatrix} - \begin{pmatrix} f_c \\ l_c \\ h_c \end{pmatrix}, \end{aligned} \quad (12)$$

the rate of change of the vectors can also be expressed as

$$\begin{aligned} \frac{D\vec{R}_W}{Dt} &= \frac{D\vec{R}_{LW}}{Dt} - \frac{D\vec{R}_L}{Dt} \\ &= \frac{d\vec{R}_{LW}}{dt} + \vec{\omega}_L \times \vec{R} - \frac{D\vec{R}_L}{Dt}, \end{aligned} \quad (13)$$

where the change of the relative position \vec{R}_{LW} in the leader's rotating reference frame is transferred to the inertial reference frame. Assume that the desired separation between leader and follower UAVs is a constant, which means f_c, l_c and h_c are all constant, i.e.,

$$\frac{D\vec{R}_L}{Dt} = \begin{pmatrix} \dot{f}_c \\ \dot{l}_c \\ \dot{h}_c \end{pmatrix} = 0. \quad (14)$$

Then, (13) can be rewritten as

$$\begin{aligned} \begin{pmatrix} \dot{f} \\ \dot{l} \\ \dot{h} \end{pmatrix} &= B_{WL} \begin{pmatrix} \dot{x}_L - \dot{x}_W \\ \dot{y}_L - \dot{y}_W \\ \dot{z}_L - \dot{z}_W \end{pmatrix} + \omega_L \times \vec{R}_{WL} \\ &= \begin{pmatrix} v_L - v_{Wx}^L \\ -v_{Wy}^L \\ -v_{Wz}^L \end{pmatrix} + \omega_L \times \vec{R}_{WL}, \end{aligned} \quad (15)$$

where v_{Wx}, v_{Wy}, v_{Wz} are the wing UAV's velocity described in the leader UAV's wind frame. The desired velocity of follower UAV can be resolved in the leader UAV's wind frame as follows:

$$\vec{V}_W^L = \begin{pmatrix} v_{Wx}^L \\ v_{Wy}^L \\ v_{Wz}^L \end{pmatrix}, \quad (16)$$

which implies that the desired velocity of follower UAV can be expressed in the NED frame as follows:

$$\vec{V}_W = \begin{pmatrix} u_{\text{ref}} \\ v_{\text{ref}} \\ w_{\text{ref}} \end{pmatrix} = B^{L \rightarrow \text{body}} \begin{pmatrix} v_{Wx}^L \\ v_{Wy}^L \\ v_{Wz}^L \end{pmatrix}, \quad (17)$$

where $B^{\text{body} \rightarrow L}$ is the transformation matrix from the UAV's body frame to the leader's wind frame.

By neglecting the roll and pitch direction rotation, the kinematic equation of motion is given by

$$\begin{pmatrix} \dot{f} \\ \dot{l} \\ \dot{h} \\ \dot{\psi} \end{pmatrix} = \begin{pmatrix} V_L - v_{Wxc}^L \\ -v_{Wyc}^L \\ -v_{Wzc}^L \\ k_\psi(\psi - \psi_{\text{ref}}) \end{pmatrix} + \begin{pmatrix} -\omega_z^L l_c + l \\ \omega_z^L f_c + f \\ 0 \\ 0 \end{pmatrix}, \quad (18)$$

$$\begin{pmatrix} u_{\text{ref}} \\ v_{\text{ref}} \\ w_{\text{ref}} \end{pmatrix} = B^{\text{body} \rightarrow L} \begin{pmatrix} v_{Wxc}^L \\ v_{Wyc}^L \\ v_{Wzc}^L \end{pmatrix}, \quad (19)$$

where $\psi_{\text{ref}}, u_{\text{ref}}, v_{\text{ref}}, w_{\text{ref}}$ are the commanded references to the autopilots, and k_ψ is the negative constant associated with the autopilot. There are four inputs, $v_{Wxc}^L, v_{Wyc}^L, v_{Wzc}^L$ and ψ_{ref} , and four outputs, $f, l, h,$ and ψ . For the outer-loop control, a good and simple idea is to use a feedback controller with a dynamic inversion to cancel the coupling terms.

3.2 Dynamic inversion control for follower UAV

If we consider only formation dynamics in the horizontal plane, the dynamic inversion control law is given by

$$\begin{aligned} \begin{pmatrix} u_{\text{ref}} \\ v_{\text{ref}} \\ w_{\text{ref}} \\ r_{\text{ref}} \end{pmatrix} &= C^{-1} \left[A_\phi \begin{pmatrix} f \\ l \\ h \\ \psi_r \end{pmatrix} + \begin{pmatrix} v_L - \omega_z^L l_c \\ \omega_z^L \\ 0 \\ 0 \end{pmatrix} \right] \\ &= C \left[A_\phi \begin{pmatrix} f \\ l \\ h \\ \psi_r \end{pmatrix} + \begin{pmatrix} v_L - \omega_z^L l_c \\ \omega_z^L \\ 0 \\ 0 \end{pmatrix} \right] \end{aligned} \quad (20)$$

with

$$C = C^{-1} = \begin{bmatrix} -\cos \psi_r & -\sin \psi_r & 0 & 0 \\ -\sin \psi_r & \cos \psi_r & 0 & 0 \\ 0 & 0 & 1 & 0 \\ 0 & 0 & 0 & 1 \end{bmatrix}, \quad (21)$$

$$A_\phi = \begin{bmatrix} k & -\omega_z^L & 0 & 0 \\ \omega_z^L & k & 0 & 0 \\ 0 & 0 & k_h & 0 \\ 0 & 0 & 0 & k_\psi \end{bmatrix}, \quad (22)$$

where $\psi_r = \psi_L - \psi_W$ is the difference between the leader UAV and follower UAV's heading angle. $\Delta r = r_L - r_W$ is the difference between the leader UAV and follower UAV's

heading angular rate, and k_f, k_l, k_h, k_ψ are the proportional control gains. The overall control structure for the follower is given in Fig.3.

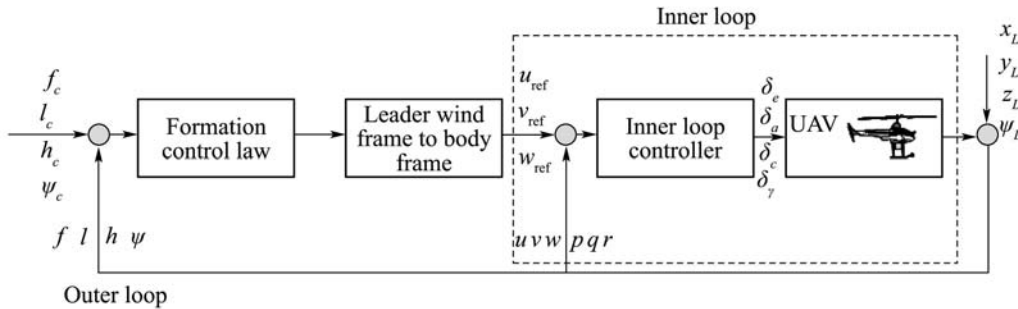


Fig. 3 The controller structure for the follower UAV.

3.3 Formation flight input constraint

As we know, a single UAV has its limitation problem for trajectory tracking, that is, an UAV cannot follow a high dynamic trajectory (see, for example, [13]). For example, when an UAV is to track a circular path (see Fig.4), the lateral movement is determined by

$$a_l = \frac{V^2}{R} = V\omega_{\text{heading}} \leq a_{\text{max}} \quad (23)$$

with V being the longitudinal ground speed of the UAV, R the radius of the circle-arc, ω_{heading} the heading rotating angular rate, a_l the lateral acceleration, and a_{max} a certain constant representing the maximum acceleration the UAV can achieve in its lateral direction.

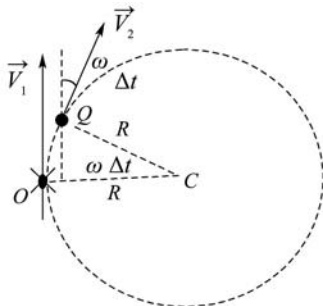


Fig. 4 The lateral flight limitation of UAV.

As the lateral acceleration, which is related to the servo deflection angle, is usually a limited constant, the velocity and heading angular rate is thus limited to be inversely proportional, which means when the velocity reaches its maximum, the heading angular rate can only reach a low limited value.

As shown in (18), to track the desired path that follows the leader UAV, the follower UAV must keep the same heading angular rate and also a velocity given by (18). This means that if the leader UAV and follower UAV are of the same model and have the same input limit, the follower UAV cannot follow the leader UAV's arbitrary maneuvers. For example, suppose the leader is turning a circle and a follower UAV is at the outside the circle, then to follow the leader UAV's flight path, the follower UAV should track a larger circle, which means it poses higher speed requirement for the follower UAV, hence the angular rate is further limited for the follower UAV. Therefore, the leader-follower mode formation flight control scheme can reach desirable

performance only under the condition that the leader UAV is performing mild maneuvers or the follower UAV has a much higher input capability. The larger the separation between the leader and the follower UAVs, the higher the input capability should be for the follower UAV.

4 Collision avoidance

UAV formation flight is a dangerous experiment. An emergency protection scheme needs to be designed to avoid collision between the formation team members. In the collision avoidance scheme, each UAV is surrounded by an imaginary space which forms a protected safe zone which no other UAV should enter. A larger space around the UAV forms its alert zone. When an UAV enters the alert zone of another UAV, a protocol for conflict resolution should be performed by both UAVs. It is important to determine the size of the safe zone. The optimal but safe size of the protected space is still an open problem and depends on factors such as speed, altitude accuracy of sensing equipment, and average human and system response times. The zones (see in [14]) are illustrated in Fig.5.

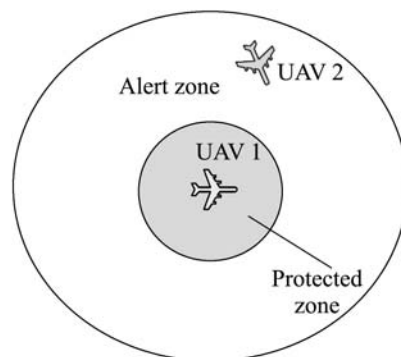


Fig. 5 Alert zone and protected zone surrounding a UAV.

There are several proposals for conflict prediction and resolution. We are interested in decentralized approaches, in which each UAV is allowed to self-optimize its own trajectory. Coordination among the UAVs is by means of maneuvers which are flight modes like heading, altitude, or speed changes for each UAV when they are in each other's alert zones. UAVs with overlapping alert zones keep each other updated about their positions. As the conflicts between UAVs depend on the relative position and velocity of the UAVs, the continuous models we use are relative models,

describing the motion of each UAV in the system with respect to the other UAV. For convenience, a relative model with its origin centered on host UAV is used. The following is an analysis based on two UAVs as depicted in Fig.6. It is to be extended to multiple UAV collision avoidance.

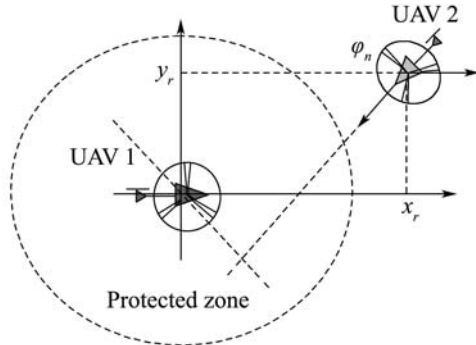


Fig. 6 Horizontal configuration of UAVs in collision avoidance.

Assume that the UAVs fly in the horizontal plane, and the pitch and roll angles, θ and ϕ , are usually around 0, a simpler relative equation can be derived as (see also [14])

$$\begin{pmatrix} x_r \\ y_r \\ z_r \end{pmatrix} = R(-\psi_1) \begin{pmatrix} x_2 - x_1 \\ y_2 - y_1 \\ z_2 - z_1 \end{pmatrix}, \quad (24)$$

$$\psi_r = \psi_2 - \psi_1 \quad (25)$$

with x_i, y_i, z_i , and ψ_i parameterizing the absolute UAV i 's position, velocity, and Euler heading angle. In local coordinates, we can derive the equations as follows:

$$\begin{pmatrix} \dot{x}_r \\ \dot{y}_r \\ \dot{z}_r \end{pmatrix} = \begin{pmatrix} v_2 \cos \psi_r - v_1 \\ v_2 \sin \psi_r \\ v_{z2} - v_{z1} \end{pmatrix} + \begin{pmatrix} -\omega_z y_r \\ \omega_z x_r \\ 0 \end{pmatrix}, \quad (26)$$

$$\dot{\psi}_r = \dot{\psi}_2 - \dot{\psi}_1 = \omega_{z2} - \omega_{z1}, \quad (27)$$

where v_1 and v_2 are the linear velocities of UAV 1 and UAV 2 projected to the horizontal plane, respectively, and v_{z1} and v_{z2} are the linear velocities of UAV 1 and UAV 2 projected to the vertical axis, respectively. Thus, the dynamics $\dot{x} = f(x, u, d)$ is described by (26) and (27) with $x = (x_r, y_r, z_r, \psi_r)^T$. The linear velocity or the heading angular velocity of UAV 1 is the control input u , and uncertain linear velocity or the heading angular velocity of UAV 2 is considered to be the disturbance d .

The threshold function $l(x)$ is defined as

$$l(x) = x_r^2 + y_r^2 + z_r^2 - \alpha_r^2, \quad (28)$$

where α_r is the threshold separation. Consider the dynamics of the UAV in one discrete state:

$$\dot{x} = f(x, u, d), \quad x(t) = x, \quad (29)$$

where $x \in \mathbb{R}^n$ describes the relative configuration of UAV 2 with respect to UAV 1, $u \in U \subset \mathbb{R}^u$ is the control input which models the actions of UAV 1, and $d \in D \subset \mathbb{R}^d$ is the disturbance input which models the actions of UAV 2. We assume that the system starts at state x at initial time t . Both U and D are known sets, but whereas the control input u may be chosen by the designer, the disturbance d is unknown, and models the uncertainty of the actions of UAV 2.

The goal is to maintain safe operation of the formation group, meaning that the group trajectories do not enter T , a ‘‘target set’’. We assume that there exists a differentiable function $l(x)$ so that $T = \{x \in \mathbb{R}^n | l(x) \leq 0\}$ and $\partial T = \{x \in \mathbb{R}^n | l(x) = 0\}$ (Tomlin et al. [14]). In (27), the control input includes velocity and three angular rates of UAV 1, the uncertain linear velocity and angular rate of UAV 2 are considered to be disturbances.

The first derivatives of the $l(x)$ can be obtained accordingly as

$$\begin{aligned} \dot{l}(x) &= x_r \dot{x}_r + y_r \dot{y}_r + z_r \dot{z}_r \\ &= -v_1 x_r + v_2 (x_r \cos \psi_r + y_r \sin \psi_r) \\ &\quad + z_r (v_{z2} - v_{z1}). \end{aligned} \quad (30)$$

Those (x_r, y_r, z_r, ψ_r) for which

$$\dot{l}(x) \leq 0 \quad (31)$$

constitute the unsafe portion.

Let us consider the linear velocity as control input only.

From (30), note the aim here is to make $\dot{l}(x)$ always greater than 0. Therefore, we first define the switching functions s_1, s_2 as

$$s_1 = x_r, \quad s_2 = z_r. \quad (32)$$

The solution is given by

$$v_1^* = \begin{cases} \underline{v}_1 & \text{if } s_1 > 0, \\ \bar{v}_1 & \text{if } s_1 < 0, \end{cases} \quad (33)$$

$$v_{z1}^* = \begin{cases} \underline{v}_{z1} & \text{if } s_2 > 0, \\ \bar{v}_{z1} & \text{if } s_2 < 0. \end{cases} \quad (34)$$

Now consider the angular velocity as control input. However, we cannot control $\dot{l}(x)$ using angular velocity only, as the cost function loses dependence on ω_1 and ω_2 at the point.

The second derivative equation gives

$$\begin{aligned} \ddot{l}(x) &= v_1^2 + v_2^2 + (v_{z2} - v_{z1})^2 - 2v_1 v_2 \cos \psi_r - \dot{v}_{z1} z_r \\ &\quad - \dot{v}_1 x_r - \omega_1 v_1 y_r + \omega_2 v_2 (y_r \cos \psi_r - x_r \sin \psi_r) \\ &\quad + \dot{v}_{z2} z_r + \dot{v}_2 (x_r \cos \psi_r + y_r \sin \psi_r), \end{aligned} \quad (35)$$

where v_i is the linear velocity of the UAV i in the horizontal plane, and v_{zi} is the linear velocity of the UAV i in the vertical axis.

As the angular velocity appears in the second derivatives of the cost function, the angular velocity as the control input can still be effective for collision avoidance in an indirect way by changing the heading angle. The switching function is defined as

$$s_3 = y_r. \quad (36)$$

Suppose the limitation for UAV 1, $v_1 \in [\underline{v}_1, \bar{v}_1]$ and $v_{z1} \in [\underline{v}_{z1}, \bar{v}_{z1}]$. The control input can be given as

$$\begin{cases} \text{if } s_3 > 0, & \omega_1 = \underline{\omega}, \\ \text{if } s_3 < 0, & \omega_1 = \bar{\omega}. \end{cases} \quad (37)$$

In a free flight, UAV 2 is also controllable. The switching function for UAV 2 can be obtained similarly as for UAV 1. In UAV 1's local coordinates, the switching function is in the format:

$$\begin{cases} s_4 = (x_r \cos \psi_r + y_r \sin \psi_r), \\ s_5 = (y_r \cos \psi_r - x_r \sin \psi_r), \\ s_6 = z_r. \end{cases} \quad (38)$$

The solution is given as

$$\begin{cases} \text{if } s_4 > 0, & v_2 = \bar{v}_2, \\ \text{if } s_4 < 0, & v_2 = \underline{v}_2, \\ \text{if } s_5 > 0, & \omega_2 = \bar{\omega}, \\ \text{if } s_5 < 0, & \omega_2 = \underline{\omega}, \\ \text{if } s_6 > 0, & v_{z2} = \bar{v}_{z2}, \\ \text{if } s_6 < 0, & v_{z2} = \underline{v}_{z2}. \end{cases} \quad (39)$$

5 Flight simulation and test results

In what follows, we present the simulation result for the proposed collision avoidance scheme and the implementation result of the formation flight with a virtual leader but with a real follower.

5.1 Collision avoidance simulation

Here we present simulation results on UAV collision avoidance using the approach described in the previous section. A scenario with two UAVs' potential collision is simulated. As shown in Figs.7 and 8, UAV 1 flies along the x-axis with a speed of 2 m/s from the original point. UAV 2 originally at $(-6, 6)$ enters into the safe zone of UAV 1 with the heading angle of $-\pi/2$ with a speed of 3 m/s. This triggers the solution in (34) and (37). The upper and lower limitations of the linear velocity of UAV 1 are 5 m/s and 0 m/s. The upper and lower limitations of the heading angular velocity of UAV 1 are -1 rad/s and 1 rad/s. Fig.7 shows both UAVs are controllable with the solution of (34), (37), and (39) executed by both UAVs, while Fig.8 shows only UAV 1 is controllable with the solution of (34) and (37) executed by UAV 1. With a sufficient size safe zone, UAV 1 is able to avoid the potential collision emergency.

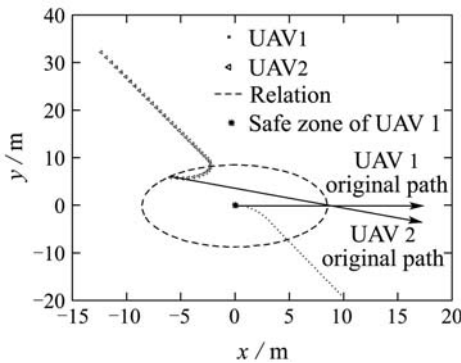


Fig. 7 Simulation result, collision avoidance (collision scenario (both UAVs are controllable)).

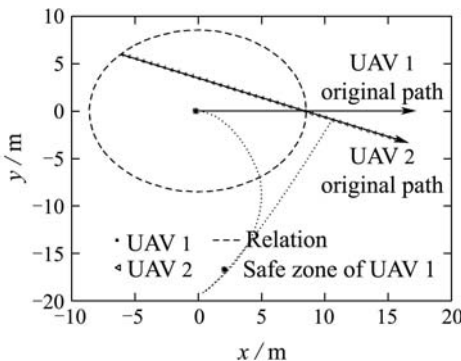


Fig. 8 Simulation result, collision avoidance (collision scenario (only UAV 1 is controllable)).

5.2 Formation flight experiment setup and result

For each UAV, we installed one wireless transceiver in the onboard control system and one wireless modem in the ground computer station for data transferring through down-link or up-link instantaneously between the on-board control system and the ground station correspondingly. The FreeWave wireless modem owns a compact structure with the weight less than 100 g, and the transmission rate can be kept at 115.2 kbps within a 20-mile range. This device has been tested on the ground under the Qnet, the particular transmission protocol used under the QNX Neutrino RTOS. Through the wireless modem and wireless transceiver, the main processing board can communicate with the ground station effectively.

Safety is a critical factor throughout the entire flight testing program. To maximize safety, a step-by-step (Hall et al. [15]) approach was used. Based on the autonomous UAV flight controller by our previous work, the flight testing experiment was designed into the following phases:

Phase 1: Virtual leader A 'virtual leader' (VL) approach was first implemented for a detailed analysis of the formation control laws prior to an actual 2-UAV formation demonstration. The use of the VL concept allowed a detailed testing of the formation control laws without the risks associated with the flight-testing of multiple UAV. Results of the 'virtual leader' testing will validate the overall design of the formation controller and confirm the performance of the on-board computer system. This experiment consisted of a single UAV tracking the trajectories of a VL, which was essentially a flight path previously recorded by one UAV. A 2-step implementation strategy was adopted for the VL flights. First the flight data to be tracked were pre-loaded on the UAV onboard computer and fed to the formation control software. After this strategy was proved successful by simulation and actual flight experiment, an additional step of beaming the VL flight data to the RF modem was performed.

Phase 2: Leader-chaser As depicted in Fig.9, the formation flight system consists of a human-piloted leader helicopter and an autonomous chase UAV that follows the lead helicopter's flight path. Airborne, the R/C UAV pilots are tasked to position their vehicle at a 'nominal' flight condition within a pre-selected 'rendezvous' area. Once at the rendezvous area, pilots of the 'follower' UAV are tasked to engage their formation controllers. As with the VL testing, the objective is to track the 'leader' UAV trajectory with a pre-selected distance for the forward, lateral, and vertical clearances set on the 'follower' UAV. As the leader UAV is flown, its trajectory is determined through an on-board GPS receiver, and these data are transmitted to the ground control station. Software at the ground control station filters this trajectory in order to generate suitable waypoints for the chase helicopter. These waypoints are used to continuously update the chase helicopter's flight plan which is then uploaded to the autopilot unit on the chase/follower UAV. After the formation mode is engaged, the 'follower' UAV is controlled with the designed formation controller, while the R/C pilot remains on standby mode in the event of an emergency. Essentially, once formation has been engaged, the 'leader' R/C pilot manually controls and directs the 'leader/follower(s)'

group. After the disengagement of formation mode, each UAV will land autonomously or under manual control.

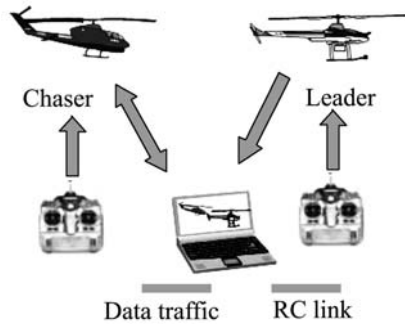


Fig. 9 Data flow in a leader-chaser flight experiment.

Phase 3: Actual formation flight Up to now, a formation flight test with a virtual leader followed by a real follower has been implemented for a detailed analysis of the formation control laws prior to an actual 2-UAV formation demonstration. Results of the virtual leader test validated the overall design of the formation controller and confirmed the performance of the on-board computer system.

This experiment consisted of a single UAV tracking the trajectories of a VL. The flight data to be tracked were pre-loaded on the ground station. The wireless modems were set to a master for ground station, a slave for the UAV helicopter, which communicate each other in dual directions. During the flight experiment, the follower UAV roughly performed path tracking. The path was dynamically scheduled through wireless communication by the ground station relative to the leader's position. The sampling period for formation information used in the implementation was 200 ms. Figs.10 and 11 show the leader UAV information with real GPS data. The virtual separation of the formation team members were set at: $l_c = 5$ m, $f_c = 5$ m, $h_c = 5$ m, which implies that the 'follower' UAV tracks the VL data from 5 meters behind, 5 meters to the right, and 5 meters above.

The results with a tracking error less than 4m clearly show that the UAV helicopter with the formation flight control law successfully completed the preset formation flight missions. The operability of the UAV helicopter is proven to be excellent.

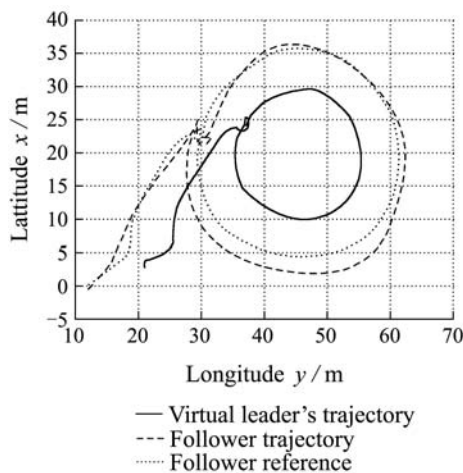


Fig. 10 Flight result on the horizontal helicopter.

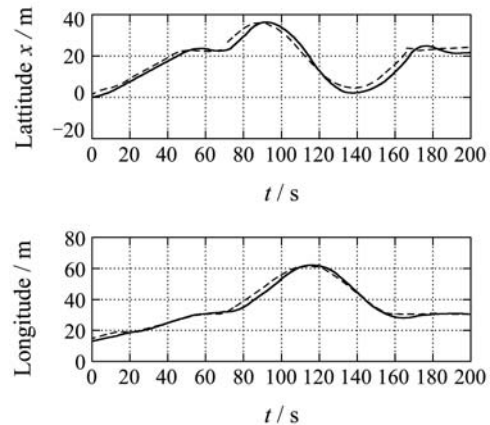


Fig. 11 Flight result in longitude and latitude (dashed line – follower trajectory; solid line – follower reference).

6 Conclusions

We have presented in this work a formation dynamic model for the follower UAV in a leader-follower formation flight full scheme. In the formation control algorithm, only the leader UAV periodically broadcasts its position and velocity to the other UAV that uses this information to maintain a fixed distance from the leader while following a prescribed mission trajectory. A special virtual leader experiment has shown that the controller is stable and has a good performance. Collision and obstacle avoidance were also studied with solutions for multiple UAV formation flight.

References

- [1] Q. Chen. Hybrid system model and overlapping decomposition for vehicle flight formation control[C]//*Proceedings of the 42nd IEEE Conference on Decision and Control*. Waterloo: Watam Press, 2004: 475 – 488.
- [2] M. J. Allen, J. Ryan, C. E. Hanson, et al. String stability of a linear formation flight control system[C]//*AIAA Guidance, Navigation and Control Conference*. Monterey, 2002: 4749 – 4756.
- [3] D. B. Edwards, T. A. Bean, D. L. Odell, et al. A leader-follower algorithm for multiple AUV formations[C]//*Proceedings of 2004 IEEE/OES Autonomous Underwater Vehicles*. New York: IEEE, 2004: 517 – 523.
- [4] F. Guilietti, L. Pollini, M. Innocenti. Autonomous formation flight[J]. *IEEE Controls System Magazine*, 2000, 20(6): 34 – 44.
- [5] D. Naffin, M. Akar, G. Sukhatme. Lateral and longitudinal stability for decentralized formation control[C]//*Proceedings of the 7th International Symposium on Distributed Autonomous Robotic Systems*. New York: Springer, 2004: 443 – 452.
- [6] P. Seiler, A. Pant, K. Hedrick. Analysis of bird formations[C]//*Proceedings of the 41st IEEE Conference on Decision and Control*. New York: IEEE, 2002: 118 – 123.
- [7] G. Cai, B. M. Chen, K. Peng, et al. Modeling and control system design for a UAV helicopter[C]//*Proceedings of the 14th Mediterranean Conference on Control and Automation*. Piscataway: IEEE, 2006: 600 – 606.
- [8] G. Cai, K. Peng, B. M. Chen, et al. Design and assembling of a UAV helicopter system[C]//*Proceedings of the 5th International Conference on Control and Automation*. Piscataway: IEEE, 2005: 697 – 702.
- [9] K. Peng, M. Dong, B. M. Chen, et al. Design and implementation of a fully autonomous flight control system for a UAV helicopter[C]//*Proceedings of the 26th Chinese Control Conference*. Beijing: Beijing University of Aeronautics & Astronautics Press, 2007: 662 – 667.

- [10] B. Kim, Y. Chang, M. Hyung. System identification and 6-DOF hovering controller design of unmanned model helicopter[C]// *Proceedings of the 2000 IEEE International Conference on Control Applications*. Sendai: Japan Society Mechanical Engineering (JSME), 2000: 1048 – 1057.
- [11] G. Larson. *Autonomous Formation Flight*[M]. Presentation to MIT 16.886 Class, 2004.
- [12] G. Campa, B. Seanor, Y. Gu, et al. NLDI guidance control laws for close formation flight[C]//*Proceedings of the 2005 American Control Conference*. New York: IEEE, 2005: 2972 – 2977.
- [13] G. Ducard, K. C. Kulling, H. P. Geering. A simple and adaptive on-line path planning system for a UAV[C]//*Proceedings of the 15th Mediterranean Conference on Control & Automation*. Piscataway: IEEE, 2007: 9 – 15.
- [14] C. Tomlin, G. J. Pappas, S. Sastry. Conflict resolution for air traffic management: A case study in multi-agent hybrid systems[J]. *IEEE Transactions on Automatic Control*, 1998, 43(4): 509 – 521.
- [15] J. K. Hall. Three dimensional formation flight control[C]// *Proceedings of the 39th IEEE Conference on Decision and Control*. Piscataway: IEEE, 2000: 364 – 369.



Ben YUN received his B.E. degree and M.E. degree from the Harbin Institute of Technology in 1997 and 1999, respectively. He is currently completing his Ph.D. program in the Department of Electrical and Computer Engineering, National University of Singapore. His research interests include control systems, flight dynamics, unmanned system, formation flight and Sensor fusion. He has been an IEEE student member since 2006.



Ben M. CHEN was born in Fuqing, Fujian, China, in 1963. He received his B.S. degree in Computer Science and Mathematics from Xiamen University, China, in 1983; his M.S. degree in Electrical Engineering from Gonzaga University, Spokane, in 1988; and his Ph.D. degree in Electrical and Computer Engineering from Washington State University, Pullman, in 1991. He was a software engineer in the South-China Computer Corporation, Guangzhou, China, from 1983 to 1986. From 1992 to 1993, he was an assistant professor in the Department of Electrical Engineering, State University of New York at Stony Brook. Since 1993, he has been with the Department of Electrical and Computer Engineering, National University of Singapore, where he is currently a professor. His current research interests are in robust control, systems theory, the development of UAV helicopter systems, and financial modeling.

He is a Fellow of IEEE and is the author/coauthor of seven research monographs including *Robust and H_∞ Control* (New York: Springer, 2000); *Linear Systems Theory: A Structural Decomposition Approach* (Boston: Birkhäuser, 2004); and *Hard Disk Drive Servo Systems* (New York: Springer, 1st Ed. 2002, 2nd Ed. 2006). He was an associate editor for *IEEE Transactions on Automatic Control*, and *Automatica*. He is currently serving as an associate editor of *Systems & Control Letters* and an editor-at-large of *Journal of Control Theory & Applications*.



Kai Yew LUM is principal research scientist at Temasek Laboratories of the National University of Singapore and, concurrently, teaching associate in the Department of Electrical and Computer Engineering. He received his Diplôme d'Ingénieur from the Ecole Nationale Supérieure d'Ingénieurs Electriciens de Grenoble, France in 1988, and his M.S. and Ph.D. from the University of Michigan, Department of Aerospace Engineering, in 1995 and 1997, respectively. He worked in the DSO National Laboratories, Singapore as junior engineer from 1990 to 1993, then as senior engineer from 1998 to 2001, specializing in control and guidance technologies. He joined the National University of Singapore in 2001. Currently, he is the principal investigator of research programmes in control, guidance and multi-agent systems. His research interests include nonlinear dynamics and control, predictive guidance, estimation, and optimization. He is a member of the IEEE Control Systems Society, AIAA, and the Instrumentation and Control Society of Singapore.



Tong H. LEE received the B.A. degree with First Class Honours in the Engineering Tripos from Cambridge University, England, in 1980, and the Ph.D. degree from Yale University in 1987. He is a professor and senior NGS fellow in the Department of Electrical and Computer Engineering at the National University of Singapore (NUS). He was a past vice-president (research) of NUS. His research interests are in the areas of adaptive systems, knowledge-based control, intelligent mechatronics, and computational intelligence. He currently holds associate editor appointments in the *IEEE Transactions on Systems, Man and Cybernetics*; *IEEE Transactions in Industrial Electronics*; *Control Engineering Practice* (an IFAC journal); and the *International Journal of Systems Science* (Taylor and Francis, London). In addition, he is the Deputy Editor-in-Chief of *IFAC Mechatronics* journal.

He was a recipient of the Cambridge University Charles Baker Prize in Engineering, the 2004 ASCC (Melbourne) Best Industrial Control Application Paper Prize, and the 2009 ASCC (Hong Kong) Best Application Paper Award. He has also co-authored five research monographs, and holds four patents (two of which are in the technology area of adaptive systems, and the other two are in the area of intelligent mechatronics).